LIQUEFIED NATURAL GAS (LNG) PLUME INTERACTION WITH SURFACE OBSTACLES

K. M. KOTHARI and R. N. MERONEY

A paper submitted to 6th International Conference on Wind Engineering, March 21-25, 1983, Australia.

CEP82-83KMK-RNM1

LIQUEFIED NATURAL GAS (LNG) PLUME INTERACTION WITH SURFACE OBSTACLES

K.M. KOTHARI and R.N. MERONEY

Fluid Mechanics and Wind Engineering Program, Colorado State University, Fort Collins, Colorado 80521 (U.S.A.)

ABSTRACT

A wind-tunnel test program was conducted on a 1:250 scale model to determine the effects of surface obstacles on the dispersion of LNG plumes. The tests were conducted with a continuous equivalent prototype LNG boiloff rate of 30 m^3/min, and 4 and 7 m/sec wind speeds. The highest concentrations were observed without any surface obstacles. The lower wind speed (4 m/sec) resulted in higher ground-level concentrations when the surface obstacle interacted with the plume. Mean concentrations measured in a neutral density plume were about three to five times smaller in magnitude than those observed with the simulated LNG plume.

INTRODUCTION

Natural gas is a highly desirable form of energy for consumption in the United States. Its conversion to heat energy for home and industrial use is achieved with very little environmental impact. Recent efforts to expand natural gas supply include the transport of natural gas in a liquid state from distant gas fields. LNG is stored and transported at about -162°C. If a storage tank were to rupture and the contents spill out, rapid boiling of the LNG would ensue, and the liberation of a potentially flammable vapor would result. Studies (ref.1,2,3,4,5) have demonstrated that the cold LNG vapor plume will remain negatively buoyant for most conditions during the dispersion of concern. Thus, it represents a ground-level hazard. This hazard extends downwind until the atmosphere has diluted the LNG vapor below the lower flammability limit (LFL), a local concentration for methane below 5 percent by volume. Some experts assume that considerable mixing takes place during gravity driven vapor spreading; whereas others assume no dilution of vapors during this stage of dispersion. None of these formulations currently incorporate the additional complications of surface obstacles. Such interference may cause additional plume dilution or temporary pooling of high gas concentrations. This paper develops an empirical appreciation of the physics of the LNG plume interaction with surface obstacles using atmospheric boundary-layer wind tunnel experiments.

MODELING OF ATMOSPHERIC BOUNDARY LAYER AND LNG PLUME

Atmospheric boundary layer simulation

The atmospheric boundary layer is the portion of the atmosphere extending from ground-level to a height within which the major exchanges of mass, momentum, and heat occur. This region of the atmosphere is described mathematically by statements of conservation of mass, momentum, and energy (ref.6). It has been determined (ref.7,8) that kinematics and dynamics of flow systems above a certain minimum Reynolds number are independent of its magnitude. Halitsky (ref.9) reported that for concentration measurements on a cube placed in a near uniform flow field the Reynolds number required for invariance of the concentration distribution over the cube surface and downwind must exceed 11,000. Because of this invariance, the equality of Reynolds number was relaxed. Since the flow scale being modeled is small the turning of the mean wind with the height is unimportant, and the Rossby number equality can be neglected. The experiments were performed with neutral atmosphere; hence, Richardson number was equal for model and prototype conditions.

Simulation of LNG plume

In addition to modeling the turbulent structure of the atmosphere, it is necessary to scale the LNG plume source conditions properly. The method of similitude (ref.10) obtains scaling parameters by reasoning that the mass, force, energy, and property ratios should be equal for both model and prototype. The dynamics of gaseous LNG plume behavior then leads to specifying equality of Froude number, volume flux ratio, and specific gravity.

The buoyancy of a LNG plume is a function of both the mole fraction of methane and temperature. If the plume entrains air adiabatically, then the plume would remain negatively buoyant for its entire lifetime. If the humidity of the atmosphere were high then the state of buoyancy of the plume will vary from negative to weakly positive. Since the adiabatic plume assumption will yield the most conservative downwind dispersion estimates, this situation was simulated. Several investigators (ref.11,12,13) have confirmed that the Froude number is the parameter which governs LNG plume spread rate, trajectory, plume size, and entrainment during initial dense plume dilution. The equality of model and prototype specific gravity was relaxed so that pure Argon gas could be used. Froude number equality was maintained by adjusting reference wind speed. Since the thermally variable prototype gas was simulated by an isothermal simulation gas, the concentration measurements observed in the model were scaled to equivalent concentrations that would be measured in the field by the relationship:

$$\chi_p = \frac{\chi_m}{\chi_m + (1 - \chi_m)\frac{T_s}{T_a}} \quad , \tag{1}$$

where,

χ_m = volume or mole fraction measured during the model test,
T_s = source temperature of LNG during prototype conditions,
T_a = ambient air temperature during field conditions, and
χ_p = volume or mole fraction in the prototype conditions.

Simulation of neutral density plume

Once geometric and kinematic similarity for the simulated atmospheric boundary layer are achieved, the additional modeling requirements for similar neutral density plumes are: equality of density ratio, and consistent scaling of all velocities. The actual LNG evaporation rate for 30 m^3/min liquid spill rate was calculated. During the neutral density plume study an equivalent volume flow rate of neutral density gas was emitted from the area source.

EXPERIMENTAL FACILITIES

Wind-tunnel

The Environmental Wind Tunnel (EWT) at Colorado State University was used for all tests performed. This tunnel incoporates special features such as adjustable ceiling, rotating turntables, transparent boundary walls, and a long test section to permit reproduction of micrometeorological behavior at large scales. Mean wind speeds of 0.10 to 12 m/sec can be obtained in the EWT. For the present set of test data, the vortex generators and a trip at the tunnel entrance were followed by 8.8 m of smooth floor to the 1:250 scaled area source model.

Model

Based on the previous atmospheric data from sites similar to that of the present idealized site it was decided that the best reproduction of the surface wind characteristics would be at a model scale of 1:250. The circular area source having an equivalent diameter of 75 m and cylindrical tanks having an equivalent height and diameter equal to 50 m were constructed from Plexiglas. The source gas, Argon or a mixture of 10 percent Ethane, 4 percent Carbon Dioxide, and 86 percent Nitrogen, was stored in a high pressured cylinder and directed through a flowmeter into the circular area source mounted in the wind-tunnel floor.

Wind profile and turbulence measurements

The velocity profiles and turbulence profiles were measured with a Thermo-Systems, Inc. (TSI) 1050 constant temperature anemometer and a TSI model 1210 hot-film probe. The calibration standard consisted of a Matheson model 8116-0154 mass flowmeter, a Yellowsprings thermistor, and a profile conditioning section fitted to the nozzle. The mass flowmeter measures mass flow rate independent of temperature and pressure. The profile conditioning section forms a flat velocity profile with very low turbulence at the nozzle exit. Incorporating a measurement of the ambient atmospheric pressure and a profile correction factor permitted calibration for wind speeds from 0.1 to 2.0 m/sec. During calibration of the single film anemometer, the anemometer voltage response values over the velocity range of interest were fit to an expression of King's law (ref.14) but with a variable exponent. The velocity sensors were mounted on a vertical traverse and positioned over the measurement location on the model. The anemometer responses were fed to analog-to-digital converter and then to a minicomputer for immediate calculation of the velocity.

Concentration measurements (LNG plume)

A rack of eight hot-wire aspirating probes was used to obtain the concentration time histories at points downwind of the spill site. These eight instantaneous concentration sensors were connected to an eight-channel TSI hot-wire anemometer system. The voltages from the TSI unit were conditioned for input to the analog-to-digital converter by a DC suppression circuit, a passive low-pass filter circuit tuned to 100 Hz, and an operational amplifier of gain five.

The basic principles governing the behavior of aspirating hot-wire probes are discussed in ref.15,16,17. A vacuum source sufficient to choke the flow through the small orifice just downwind of the sensing element was applied. This wire was operated in a constant temperature mode at a temperature above that of the ambient air temperature. A feedback amplifier maintained a constant overheat resistance through adjustment of the heating current. A change in output voltage from this sensor circuit corresponds to a change in heat transfer between the hot-wire and sampling environment. The heat transfer rate from a hot-wire to a gas flowing over it depends primarily upon the wire diameter, the temperature difference between wire and gas, thermal conductivity and viscosity of gas, and gas velocity. For a wire in an aspirated probe with a sonic throat, the gas velocity can be expressed as a function of the ratio of the probe cross-sectional area at the wire position to the throat area, the specific heat ratio, and the speed of sound in the gas. The latter two parameters as well as the thermal conductivity and viscosity of the gas are function of composition and temperature. Hence, for a fixed geometry and wire

temperature, the heat transfer rate or the related voltage change across the wire is a function of only the gas composition and temperature. Since all tests performed were in an isothermal flow, the wire's response was a function of gas composition only.

Concentration measurements (neutral density plume)

The experimental measurements of concentration with neutral density source were performed with a gas chromatograph having a flame ionization detector (FID). The electrical conductivity of a gas is directly proportional to the concentration of charged particles within the gas. The ions in this case are formed by the sample gas mixed with hydrogen and then burned with air. The ions and electrons formed enter an electrode gap and decrease the gap resistance. The resulting voltage drop is amplified by an electrometer and fed to an integrator.

The tracer gas sampling system consisted of a series of fifty 30 cc syringes mounted between two circular aluminum plates. A variable-speed motor raises a third plate, which in turn raises all syringes simultaneously. A set of check valves and tubings were connected such that airflow from each sampling point passes over the top of each designated syringe. When the syringe plunger is raised, a sample from the tunnel is drawn into each syringe.

TEST PROGRAM

The goal of the test series was to determine the effect of surface obstacles on the dispersion of LNG and neutral density plumes. All tests were conducted at an equivalent continuous LNG spill rate of 30 m^3/min. Two wind speeds, 4 and 7 m/sec at 10 m equivalent height, with neutral atmospheric stability were investigated. The experiments were performed with a single cylindrical model tank at a scale ratio of 1:250.

A right-hand coordinate system with origin at the center of area source was utilized. Configuration 1 is the plane area source case. Ground-level concentration measurements were performed for all tests. Configurations 2 to 8 are described in Figure 1. A summary of the test program identifying run numbers, prototype wind speeds, various configuration numbers, and source density is given in Table 1. The model wind speed and flow rate were calculated using equality of Froude number and volume flow rate, respectively.

RESULTS AND DISCUSSION

Approach velocities

The approach flow velocity profiles were measured at the location of the area source center, 8.9 m from the tunnel entrance. The representative mean

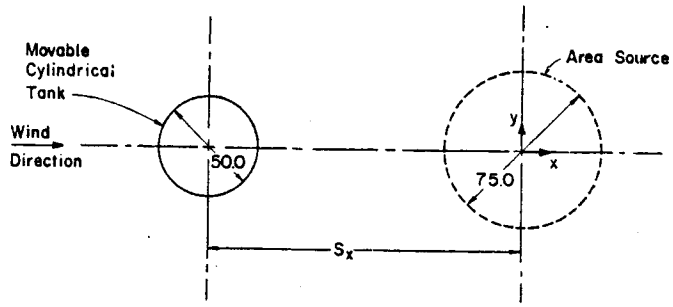

Fig. 1. Configurations 2 to 8 identification.

TABLE 1 Summary of tests.

Configuration Number	Source Density-Neutral				Source at Specific Gravity of LNG at Boiloff Temperature			
	Prototype Wind Speed @ 10 m height	Run Number	Prototype Wind Speed @ 10 m height	Run Number	Prototype Wind Speed @ 10 m height	Run Number	Prototype Wind Speed @ 10 m height	Run Number
1		1		23		45		67
2		2		24		46		68
3		3		25		47		69
4	4.0 m/sec	4	7.0 m/sec	26	4.0 m/sec	48	7.0 m/sec	70
5		5		27		49		71
6		6		28		50		72
7		7		29		51		73
8		8		30		52		74

Note: 1. LNG boiloff rate from area source = 30 m^3/min.
2. Neutral density source runs were performed with the equivalent amount of vapor generation from 30 m^3/min LNG, but with neutral density.

velocity and turbulence profiles are displayed in Figure 2. The average value of the velocity profile power-law exponent was 0.22. The average values of the prototype frictional velocity, u_*, were 0.25 m/sec and 0.44 m/sec corresponding to prototype wind speeds of 4 and 7 m/sec. The average value of the surface roughness parameter, z_o, for prototype conditions was 4 cm.

Concentration measurement results

This paper describes only the experimental measurements of LNG and neutral density plume dispersion in the wake of a single cylindrical obstacle. The additional experiments with added tanks, buildings, and a shelterbelt are described by Kothari et al. (ref.3). The neutral density plume results are presented as mean concentrations, whereas LNG plume data are given in both mean concentrations and peak concentrations.

Figures 3 and 4 show the plots of ground-level mean concentration versus downwind distance for neutral density and LNG source gas, respectively. The highest concentrations were observed without any surface obstacle. The surface obstacle generates excess turbulence intensity (ref.18,19,20,21,22) and hence accelerate plume dilution. For the unobstructed case the maximum concentrations were observed with the higher wind speed, but the lower wind speed resulted in higher ground-level concentrations when the surface obstacle

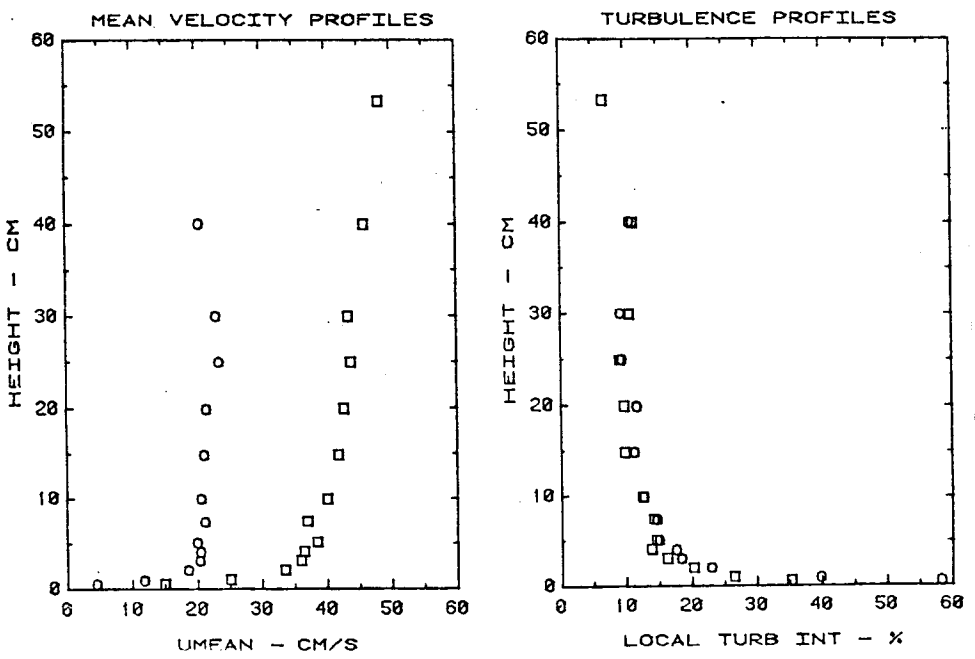

Fig. 2. Model mean velocity and turbulence intensity profiles.

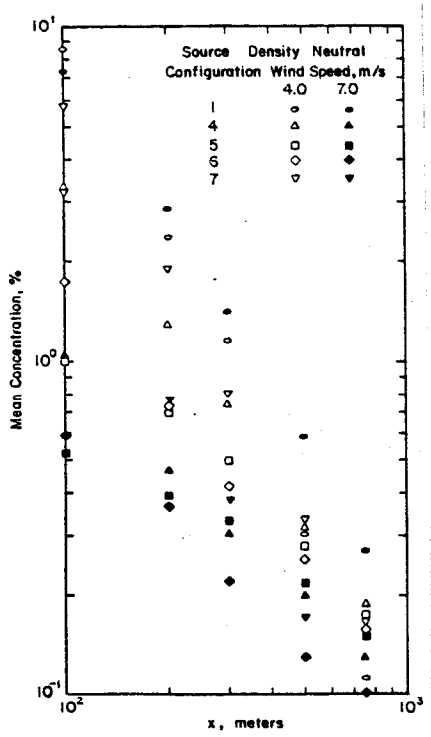

Fig. 3. Mean concentration vs. x (neutral density plume).

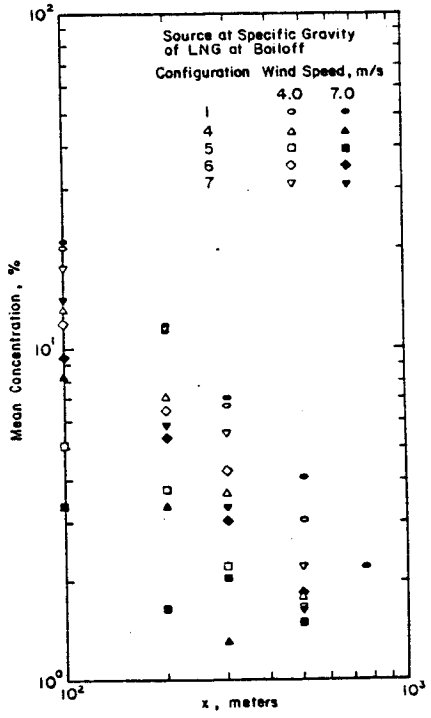

Fig. 4. Mean concentration vs. x (LNG plume).

interacted with the plume. The mean concentrations measured with the neutral density plumes were about 3 to 5 times smaller in magnitude than those observed with LNG plumes. With the cylindrical tank located upstream of the spill area, the initial dilution (measured at 100 m downwind) for LNG plume was generally 2

to 3 times smaller than that for the neutral plume data. Even with the excess turbulence generated by the presence of the cylindrical tank the entrainment of air into the heavier LNG plume was less than that for the neutral density plume. Indeed, even under the influence of the wake of cylindrical tank, it is important to account for the initial gravity spread of the LNG plume. With the cylindrical tank upstream but close to the spill area the highest plume dilution was observed. Concentration isopleths for selected runs are displayed in Figures 5 through 14. Figure 15 shows the plots of the maximum downwind distance for given ground-level concentrations versus the displacement of the cylindrical tank for various wind speeds. This figure also indicates the downwind distance for a given ground-level concentration for no obstacle case.

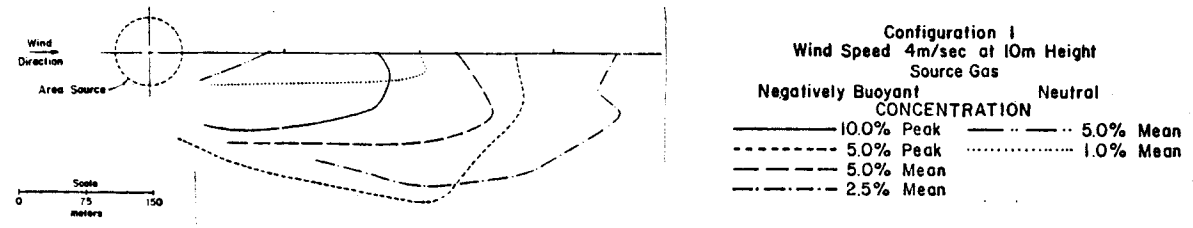

Fig. 5. Concentration isopleths for configuration 1, wind speed 4 m/sec.

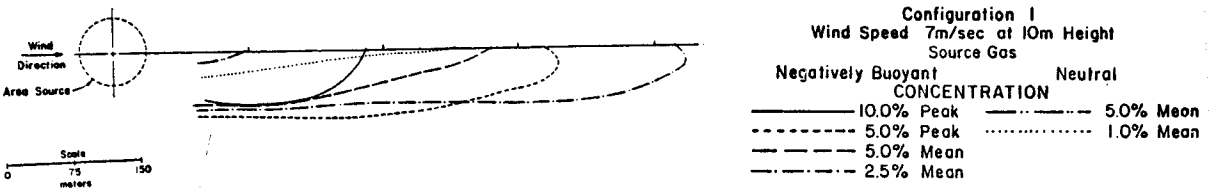

Fig. 6. Concentration isopleths for configuration 1, wind speed 7 m/sec.

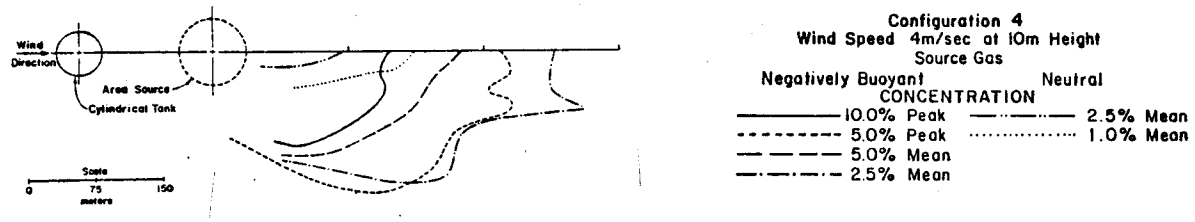

Fig. 7. Concentration isopleths for configuration 4, wind speed 4 m/sec.

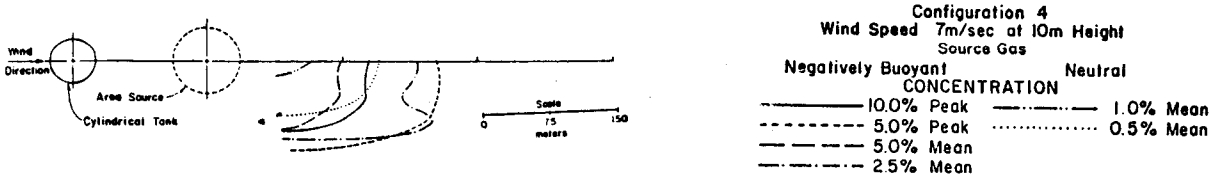

Fig. 8. Concentration isopleths for configuration 4, wind speed 7 m/sec.

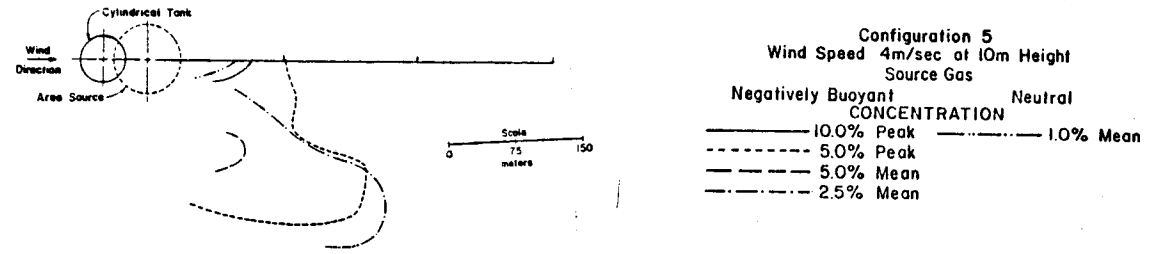

Fig. 9. Concentration isopleths for configuration 5, wind speed 4 m/sec.

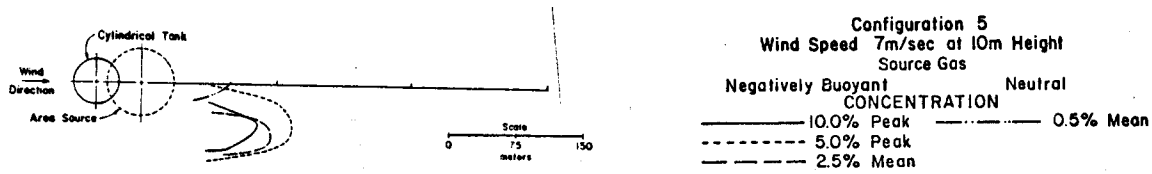

Fig. 10. Concentration isopleths for configuration 5, wind speed 7 m/sec.

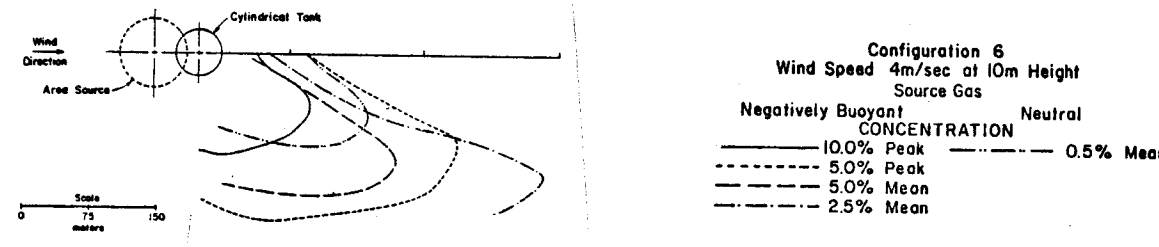

Fig. 11. Concentration isopleths for configuration 6, wind speed 4m/sec.

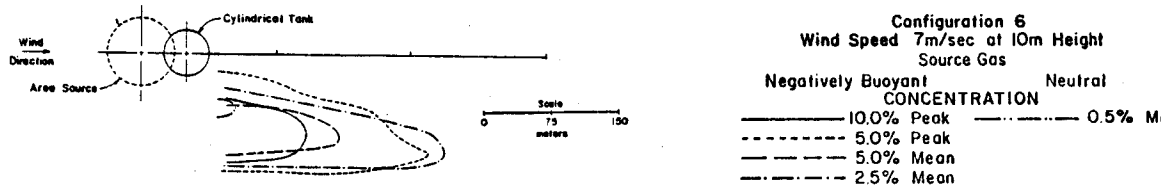

Fig. 12. Concentration isopleths for configuration 6, wind speed 7 m/sec.

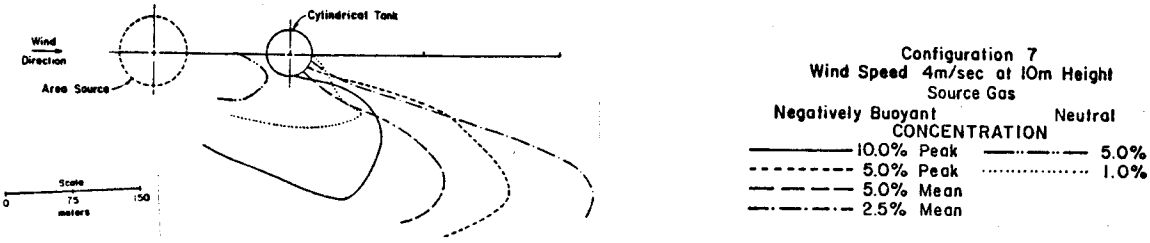

Fig. 13. Concentration isopleths for configuration 7, wind speed 4 m/sec.

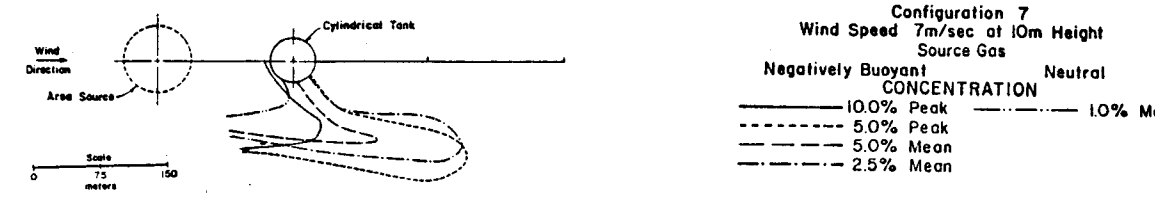

Fig. 14. Concentration isopleths for configuration 7, wind speed 7 m/sec.

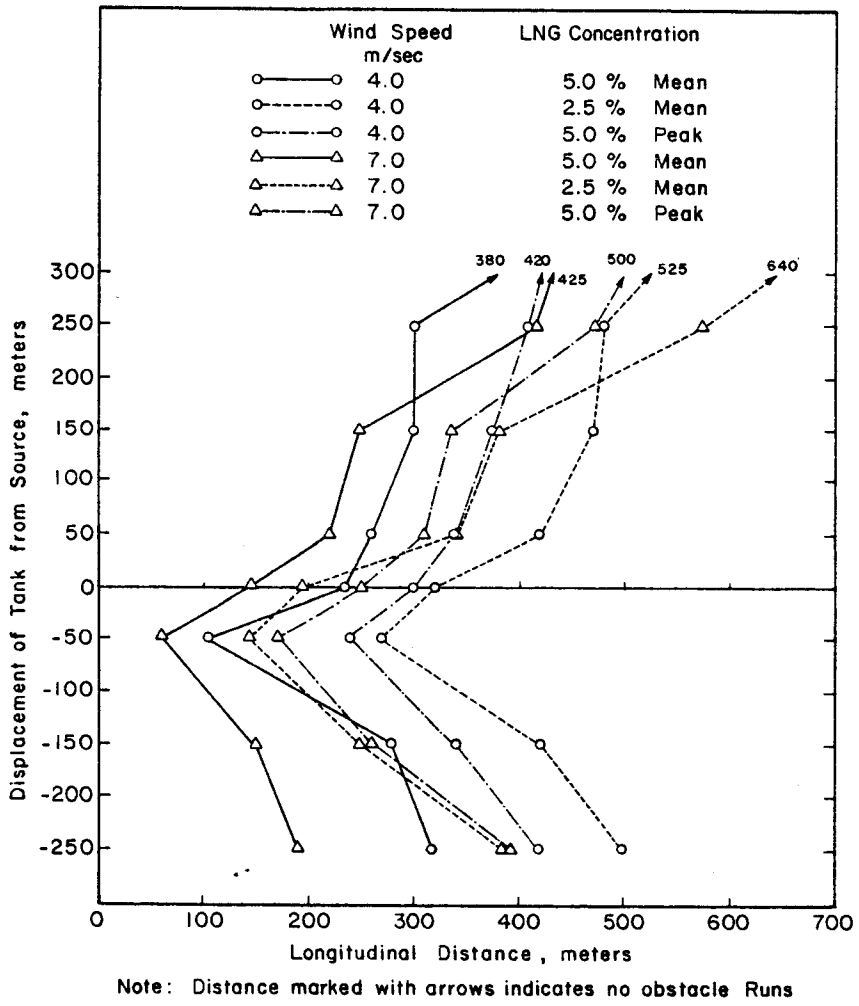

Fig. 15. Maximum downwind distance for given concentrations versus displacement of the cylindrical tank.

At lower wind speeds, plume spread is larger. This results in shorter LFL distances for the plane area source (Figures 5, 6, and 15). Configurations where the plume is affected by the surface obstacles gave longer LFL distances at lower wind speed. The LNG plume tends to have its maximum concentration off the centerline. This deviation for configuration 1 is attributed to plume meandering from the wind-tunnel centerline due to a slight lateral nonuniformity of the flow. However, for the cylindrical tank interaction cases, the deviation is caused by the following factors: (1) higher turbulence intensity in the wake of the tank which results in higher entrainment and correspondingly lower concentration in the wake region, (2) the presence of horseshoe vortices with their axis in the longitudinal direction on either side of the obstacle (Kothari et al. (ref.22)) which deflect the ambient air downward from the top of the turbulent boundary layer along the centerline of the obstacle, and (3) the defection of the plume laterally by the surface obstacle.

ACKNOWLEDGMENT

The research was performed under Contract Number 5014-352-0203 for the Environment and Safety Department of the Gas Research Institute whose financial assistance is gratefully acknowledged.

REFERENCES

1. American Gas Association, LNG Safety Program, Interim Report on Phase II Work, Report on American Gas Association Project IS-3-1, Battelle Comubus Laboratories, 1974.
2. D.E. Neff, R.N. Meroney, and J.E. Cermak, Wind Tunnel Study of Negatively Buoyant Plume Due to LNG Spill, Colorado State University Report No. CER76-77DEN-RNM-JEC22, 1976, p. 241.
3. K.M. Kothari, R.N. Meroney, and D.E. Neff, LNG Plume Interaction with Surface Obstacles, Gas Research Institute Report No. GRI 80/0095, 1981, p. 140.
4. K.M. Kothari and R.N. Meroney, Accelerated Dilution of LNG Plumes with Fences and Vortex Generators, Gas Research Institute Report, No. 81/0074, 1982.
5. R.N. Meroney, D.E. Neff, J.E. Cermak, and M. Megahed, Dispersion of Vapor from LNG Spills - Simulation in a Meteorological Wind Tunnel, Colorado State University Report No. CER76-77RNM-DEN-JEC-MM57, 1977, p. 151.
6. J.E. Cermak, Applications of Fluid Mechanics to Wind Engineering, A Freeman Scholar Lecture, Journal of Fluid Engineering, Vol. 97, Ser. 1, No. 1, 1975, pp. 9-38.
7. H. Schlichting, Boundary Layer Theory, McGraw-Hill, 1968.
8. D. Zoric and V. A. Sandborn, Similarity of Large Reynolds Number Boundary Layers, Boundary-Layer Meteorology, Vol. 2, No. 3, 1972, pp. 326-333.
9. J. Halitsky, Validation of Scaling Procedures for Wind Tunnel Modeling of Diffusion Near Buildings, New York University Report No. TR-69-8, 1969.
10. S.J. Kline, Similitude and Approximation Theory, McGraw-Hill, 1965, p. 229.
11. G.J. Boyle and A. Kneebone, Laboratory Investigation into the Characteristics of LNG Spill on Water: Evaporation, Spreading and Vapor Dispersion, Shell Research Ltd., March 1973.
12. F.T. Bodurtha, Jr., The Behavior of Dense Stack Gases, Journal of APCA, Vol. 11, No. 9, 1961, pp. 431-437.
13. A.P. van Ulden, On the Spreading of a Heavy Gas Released Near the Ground, Loss Prevention and Safety Promotion Seminar, Delft, Netherlands, 1974, p. 6.
14. V.A. Sandborn, Resistance Temperature Transducers, Metrology Press, 1972, p. 545.
15. P.L. Blackshear, Jr., and L. Fingerson, Rapid Response Heat Flux Probe for High Temperature Gases, ARS Journal, November 1962, pp. 1709-1715.

16. G.L. Brown and M.R. Rebollo, A Small, Fast Response Probe to Measure Composition of a Binery Gas Mixtures, AIAA Journal, Vol. 10, No. 5, 1972, pp. 649-752.
17. W.H. Kuretsky, On the Use of an Aspirating Hot-Film Anemometer for the Instantaneous Measurement of Temperature, Thesis, Master of Mechanical Engineering, University of Minnesota, Minneapolis, Minnesota, 1967.
18. K.M. Kothari, Stably Stratified Building Wakes, Ph.D. Dissertation, Civil Engineering Department, Colorado State University, Fort Collins, Colorado, 1979, p. 142.
19. H.G.C. Woo, J.A. Peterka, and J.E. Cermak, Wind Tunnel Measurements in the Wakes of Structures, Colorado State University Report No. CER75-76HGCW-JAP-JEC40, 1976.
20. J.P. Castro and A.G. Robins, The Effects of a Thick Incident Boundary Layer on the Flow Around a Small Surface Mounted Cube, Central Electricity Generating Board Report No. R/M/N795, England, 1975.
21. J. Counihan, An Experimental Investigation of the Cube Behind a Two-Dimensional Block and Behind a Cube in a Simulated Boundary Layer Flow, Central Electricity Generating Board Report No. RD/L/N115/71, England, 1971.
22. K.M. Kothari, R.N. Meroney, and J.A. Peterka, The Flow and Diffusion Structure in the Wakes of Cylindrical Obstacles, 4th U.S. National Conference on Wind Engineering Research, Seattle, Washington, 26-29 July, 1981.